Analysis of one-end-pumped Yb^{3+}-doped gain guided and index antiguided fiber laser

**E. Zhou · B. Zhao · X. Wang · Y. Wang · W. Wei ·
B. Peng**

Abstract The one-end-pumped Yb^{3+}-doped gain guided and index antiguided (GG+IAG) fiber laser is analyzed with a rate equation model. By solving propagation rate equations, the pump and signal, the gain coefficients and other characteristics are obtained. Computation results show that a properly designed Yb^{3+}-doped GG+IAG fiber laser can provide a large-mode laser with a short length. The most important issue addressed is the way of controlling the fiber laser length.

1 Introduction

High power fiber lasers have important applications in advanced manufacturing industry, national defense and after inertial confinement fusion (after-ICF). The major limitations to high powers in conventional single-mode fibers are the onsets of nonlinear optical effects. Gain-guided and in-

dex antiguided (GG+IAG) fiber with a negative step refractive index between the core and cladding [1–3] is found to be a new configuration. It can deliver robust large single mode and avoid high power density to cause nonlinear optical effects. Therefore, a new way of obtaining a high power fiber laser may be paved. Flashlamp-pumped [4] and laser diode-pumped [5] Nd^{3+}-doped GG+IAG fiber lasers were demonstrated for the first time in 100–200 μm core with single transverse mode up to several times their thresholds.

In this paper, we report an analytical model for a one-end-pumped Yb^{3+}-doped GG+IAG fiber laser. The model is based on a set of propagation rate equations which are valid for a quasi-three-level system (e.g. Yb^{3+} emitting in the range 1040–1100 nm). By solving propagation rate equations, the pump and signal, the gain coefficients and other characteristics are obtained.

In Sect. 2, the rate equations for a one-end-pumped Yb^{3+}-doped GG+IAG fiber laser are depicted. Section 3 describes the approximate analytical solutions for the pump when it is launched at one end of the fiber. Section 4 illustrates the computational results for the signal and other characteristics of the Yb^{3+}-doped GG+IAG fiber laser. Finally, some concluding remarks are given in Sect. 5.

E. Zhou · W. Wei (✉)
Department of Optical Science and Engineering, Fudan
University, Shanghai 200433, P.R. China
e-mail: iamww@fudan.edu.cn

B. Zhao · Y. Wang · B. Peng (✉)
State Key Laboratory of Transient Optics and Photonics, Xi'an
Institute of Optics and Precision Mechanics, The Chinese
Academy of Sciences, Xi'an 710119, P.R. China
e-mail: bpeng@opt.ac.cn

X. Wang
The School of Physical Electronics, University of Electronic
Science and Technology of China, Sichuan 610054, P.R. China

W. Wei · B. Peng
Institute of Advanced Materials, Nanjing University of Posts
and Telecommunications, Nanjing 210003, P.R. China

2 Theoretical analysis

Figure 1 shows the way of a ray passing through GG+IAG fiber. Unlike conventional fiber, the GG+IAG fiber's core has a lower refractive index than the surrounding cladding. Since total internal reflection does not occur at the core–cladding interface, such a fiber cannot support conventional index-guided modes. Light generated in the core of the fiber leaks out to the cladding, though a small fraction of trapping occurs by grazing angle reflection. However, the leakage can

be compensated by signal amplification in the core, leading to different thresholds for specific waveguide modes. With the proper threshold as described in [6], the GG+IAG fiber can propagate a robust single mode.

A set of time-independent steady-state rate equations to be solved for the GG+IAG fiber laser is given by (1) to (3) from [7], where $P_p^{\pm}(z)$ and $P_s^{\pm}(z)$ are the pump and signal powers, propagating in the positive and negative z-directions (noted by plus and minus superscripts, respectively). Γ_p and Γ_s are pump and signal field overlaps, and v_p and v_s are the pump and signal frequencies, corre-

spondingly. A is the cross-sectional area of the core, and the positive coefficients α_p and α_s represent the scattering losses for the pump and signal. N is the concentration of dopant Yb^{3+}. $N_1(z)$ and $N_2(z)$ are the lower and upper lasing level population densities, with τ being the spontaneous lifetime of $N_2(z)$. The relation $N = N_1(z) + N_2(z)$ is used to eliminate $N_1(z)$ from the equations mentioned above. The functions $\sigma_a(\lambda)$ and $\sigma_e(\lambda)$ are the absorption and emission cross sections. Furthermore, in (1) to (3), $\sigma_{ep} \equiv \sigma_e(\lambda_p)$, $\sigma_{ap} \equiv \sigma_a(\lambda_p)$ and the parameter h is Planck's constant.

$$\frac{N_2(z)}{N} = \frac{\frac{(P_p^+(z)+P_p^+(z))\sigma_{ap}\Gamma_p}{hv_pA} + \frac{\Gamma_s\sigma_a(\lambda_s)(P_s^+(z)+P_s^+(z))}{hv_sA}}{\frac{(P_p^+(z)+P_p^+(z))(\sigma_{ap}+\sigma_{ep})\Gamma_p}{hv_pA} + \frac{1}{\tau} + \frac{\Gamma_s(\sigma_a(\lambda_s)+\sigma_e(\lambda_s))(P_s^+(z)+P_s^+(z))}{hv_sA}}, \tag{1}$$

$$N = N_1(z) + N_2(z), \tag{1'}$$

$$\pm\frac{dP_p^{\pm}(z)}{dz} = -\Gamma_p\{\sigma_{ap}N - (\sigma_{ap}+\sigma_{ep})N_2(z)\}P_p^{\pm}(z) - \alpha_pP_p^{\pm}(z) - l_pP_p^{\pm}(z), \tag{2}$$

$$\pm\frac{dP_s^{\pm}(z)}{dz} = \Gamma_s[(\sigma_e(\lambda_s)+\sigma_a(\lambda_s))N_2 - \sigma_a(\lambda_s)N]P_s^{\pm}(z) - \alpha_sP_s^{\pm}(z) - l_sP_s^{\pm}(z). \tag{3}$$

Because the GG+IAG fiber structure is a negative step refractive index distribution, to (2) and (3) should be added mode-dependent leakage compared to the rate equations of a conventional fiber laser. For strongly GG+IAG fiber, the leakage losses l_p and l_s are equal to the corresponding threshold gain coefficients for different modes [3]:

$$g_{th}^{01} \approx \frac{1}{k_0^2a^3}\sqrt{\frac{133.8}{-2n_0^3\Delta n}}, \tag{4}$$

$$g_{th}^{11} \approx \frac{1}{k_0^2a^3}\sqrt{\frac{862.2}{-2n_0^3\Delta n}}, \tag{5}$$
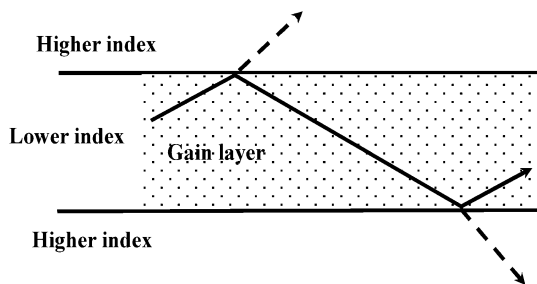

Fig. 1 Transfer way of ray in GG+IAG fiber

where k_0 is the vacuum wave number and a is the core radius of the GG+IAG fiber. n_0 and Δn are the fundamental refractive index and negative index step, correspondingly.

Equations (1) to (3) are to be solved subject to the boundary conditions posed by the reflectors:

$$P_s^+(0) = R_1P_s^-(0), \tag{6a}$$

$$P_s^-(L) = R_2P_s^+(L), \tag{6b}$$

$$P_p^-(L) = R_3P_p^+(L), \tag{6c}$$

where R_1 and R_2 are the signal power reflectivities at $z = 0$ and $z = L$, and R_3 is the pump power reflectivity at $z = L$ accordingly.

For laser oscillation to occur in a resonator formed by two mirrors of reflectivities R_1 and R_2 at the ends of a fiber of length L having losses α_{osc} per unit length, the oscillation threshold is given by

$$g_{th}^{osc} = \frac{-\ln(R_1R_2)}{2L} + \alpha_{osc}. \tag{7}$$

Here α_{osc} is the loss in the resonator and L is the fiber length. Considering the steps required to make a lowest-order single-mode laser based on the GG+IAG concept, it is important that no laser oscillations take place before the gain is sufficient to enable propagation of the LP_{01} mode of

the core. Thus, the threshold gain of laser oscillation should be

$$g_{th}^{01} < g_{th}^{osc}. \tag{8}$$

However, to ensure that only the LP$_{01}$ mode oscillates, we require that the total gain be less than that of the LP$_{11}$ mode [6]:

$$g_{tot}^{osc} = g_{th}^{osc} + g_{th}^{01} < g_{th}^{11}. \tag{9}$$

3 Solution

Firstly, we assume that $\sigma_{ep} \cong 0, \sigma_a(\lambda_s) \ll \sigma_e(\lambda_s)$ and $N_2(z) \ll N$ everywhere along the fiber. These assumptions are mostly suitable for quasi-three-level systems (such as Yb^{3+}) [8]. Meanwhile, if the gain coefficient is higher than g_{th}^{osc}, there would be a pump and signal mode propagating in the GG+IAG fiber.

Under these conditions, (1) to (3) are significantly simplified [8].

$$\pm \frac{dP_p^{\pm}(z)}{dz} = -\Gamma_p N \sigma_{ap} P_p^{\pm}(z) - \alpha_p P_p^{\pm}(z)$$

$$- \frac{1}{k_{0p}^2 a^3} \sqrt{\frac{133.8}{-2n_0^3 \Delta n}} P_p^{\pm}(z), \tag{10}$$

$$\pm \frac{dP_s^{\pm}(z)}{dz} = g_s P_s^{\pm}(z) - \alpha_s P_s^{\pm}(z)$$

$$- \frac{1}{k_{0s}^2 a^3} \sqrt{\frac{133.8}{-2n_0^3 \Delta n}} P_s^{\pm}(z), \tag{11}$$

$$g_s \cong \frac{\frac{N\Gamma_p \sigma_{ap} P_p(z)}{(v_p/v_s)(hv_s A/\Gamma_s \sigma_e(\lambda_s)\tau)} - N\Gamma_s \sigma_a(\lambda_s)}{1 + [P_s^+(z) + P_s^+(z)]/(hv_s A/\Gamma_s \sigma_e(\lambda_s)\tau)}, \tag{12}$$

where k_{0p} and k_{0s} are vacuum wave numbers of the pump and signal and g_s is the gain coefficient of the signal. In this article, the pump power is injected at $z = 0$. Assuming that $R_3 = 0$, $P_p^-(z)$ is removed and $P_p^+(z)$ is replaced by $P_p(z)$. The pump power is analytically integrated to yield

$$P_p(z)$$

$$= P_p(0) \exp\left[-\left(\Gamma_p N \sigma_{ap} + \alpha_p + \frac{1}{k_{0p}^2 a^3} \sqrt{\frac{133.8}{-2n_0^3 \Delta n}}\right)z\right], \tag{13}$$

while $P_s^{\pm}(z)$ will be given by computation.

4 Results and discussion

All parameters used for a one-end-pumped Yb^{3+}-doped GG+IAG fiber laser are given in Table 1, which come from
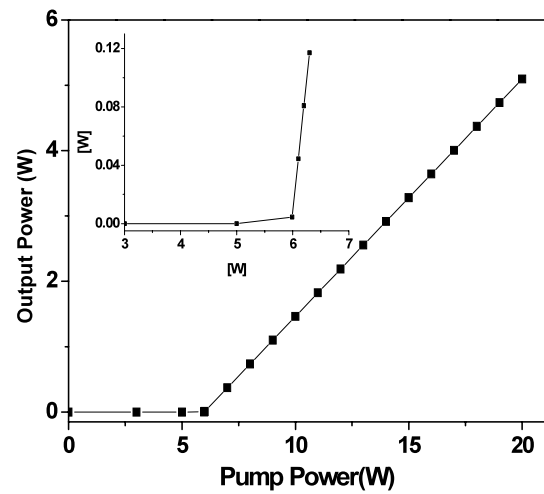

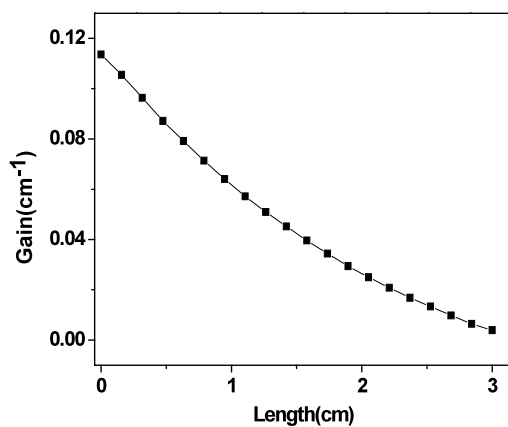**Fig. 2** Output power as a function of the pump power of Yb^{3+}-doped GG+IAG fiber laser

Table 1 The parameters used in Yb^{3+}-doped GG+IAG fiber laser

Parameter	Value
Γ_p	0.15
Γ_s	0.6
α_p	1.94×10^{-3} cm^{-1}
N	4.67×10^{20} cm^{-3}
a	0.01 cm
n_0	1.57318
Δn	–0.00094
σ_{ep}	6.76×10^{-22} cm^2
α_s	5×10^{-5} cm^{-1}
$\sigma_a(\lambda_s)$	1.4×10^{-23} cm^2
τ	1×10^{-3} s
$\sigma_e(\lambda_s)$	6.76×10^{-21} cm^2
A	3.14×10^{-4} cm^2
L	3 cm
α_{osc}	5%
R_1 at 1053 nm	1
R_2 at 1053 nm	0.75
R_3 at 980 nm	0

the Yb^{3+}-doped silicate glass of our group (Xi'an Institute of Optics and Precision Mechanics, Chinese Academy of Sciences). We also consider the case with a pump power of $P_p(0) = 20$ W injected into the fiber laser at $z = 0$. For computing the signal power, the Runge–Kutta algorithm combined with the Newton–Raphson iteration method has been adopted [9]. Then, the output power is given by $P_{out} = P_s^+(L)(1 - R_2)$ (shown in Fig. 2), emerging from the $R_2 = 0.75$ mirror, as a function of pump power P_p. Lasing threshold is about $P_p(0) = 5.9$ W (see inset) and the linear increase of output power with the pump is obtained. The
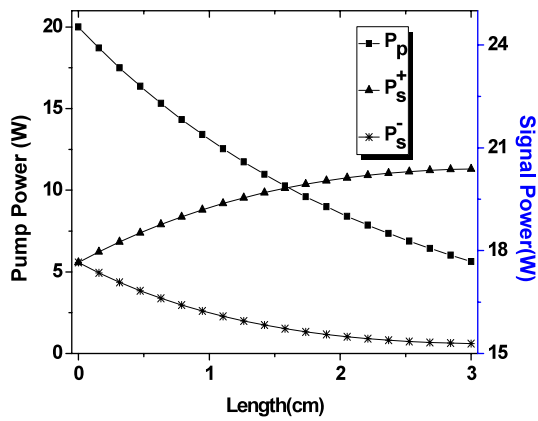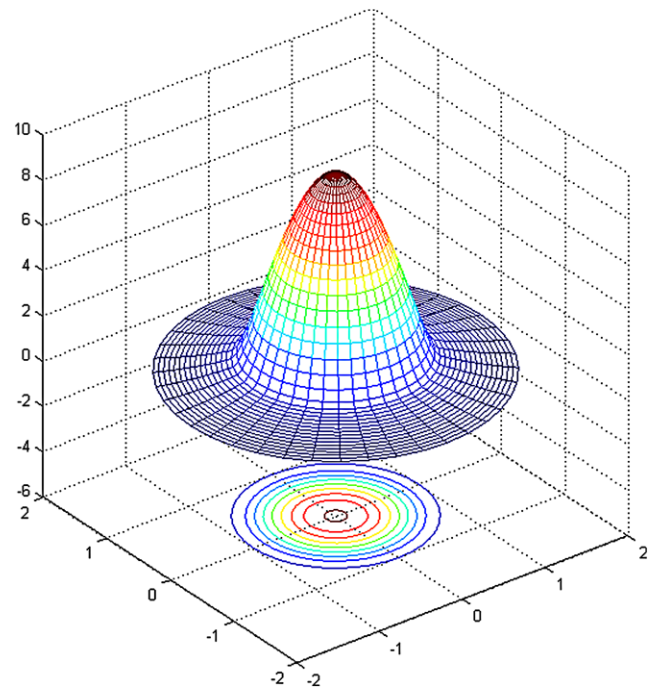
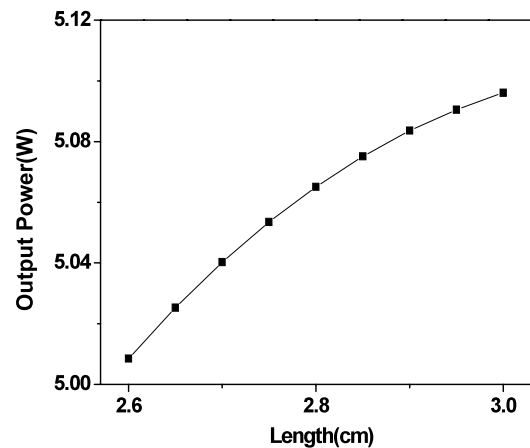**Fig. 3** Pump and signal powers vs the position along the GG+IAG fiber laser

**Fig. 4** Gain vs the position along the GG+IAG fiber laser

Fig. 5 Field distribution on the normalized transverse section of GG+IAG fiber laser

Fig. 6 Output power of GG+IAG fiber as a function of the fiber laser length

result is similar to the experimental observations in [10]. The slope efficiency of 36.3% is achieved with respect to the launched pump power. Owing to the leakage, the threshold of a Yb^{3+}-doped GG+IAG fiber laser is higher than a conventional one. However, it ensures a robust single-mode output. The characteristics of the fiber laser could ensure single-mode and high-power output, but the higher threshold is the trade-off. Meanwhile, optimizations could be used to improve the slope efficiency, such as by increasing R_3 [11].

The variation of pump and signal powers along the fiber laser length of Yb^{3+}-doped GG+IAG fiber is described in Fig. 3. Because of high absorption and leakage, the absorption length of GG+IAG fiber is shorter than that of conventional fiber. When the fiber length is 3 cm, the pump power of 71.8% has been absorbed. The effective gain coefficient of the signal g_s' (see Appendix) along the length is sketched in Fig. 4. We can see that the effective gain coefficient decreases sharply. It almost approaches zero when the fiber length is equal to 3 cm. If the single-mode operation in GG+IAG fiber is intended to be preserved, the effective gain coefficient should be in the region $0 < g_s' < g_{th}^{11} - g_{th}^{01}$. Table 1 shows that g_s' satisfies the condition $0 <$

$g_s' < 0.1179$ cm^{-1}. Neither too long nor too short length of GG+IAG fiber can keep the single-mode operation. Meanwhile, we also consider g_{th}^{osc} (the oscillation threshold) according to (8) and (9). Therefore, the fiber length of 2.6–3.0 cm can preserve robust single mode output. The single mode field distribution can therefore be evaluated and is shown in Fig. 5 [1].

Figure 6 plots the output power of a Yb^{3+}-doped GG+IAG fiber laser as a function of the laser length. The optimum fiber length is around 3 cm and the output power is 5.1 W. It is noted, however, that if the fiber length was outside the range 2.6–3.0 cm, the mode field will be non-
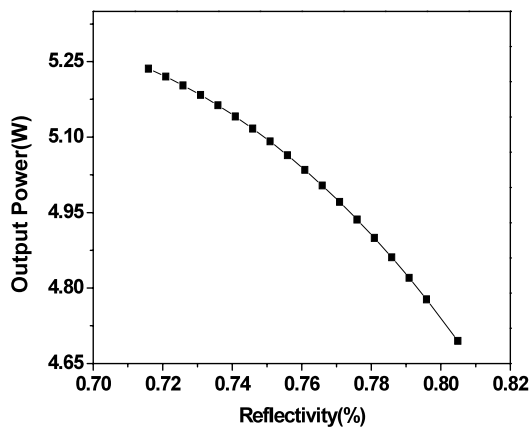
Fig. 7 The output power vs reflectivity R_2

single-mode, although the laser is also operational [6]. Consequently, an accurate length control should be emphasized.

It is detected that the output power of the GG+IAG laser changes with the variation of the reflectivity R_2. Figure 7 shows that reflectance at the output end varies; so does the output lasing power. It can also be seen that the laser reaches the maximum output when the reflectivity is around 71%. According to (8) and (9), there will no single mode laser operation if the reflectivity extends outside 71–81%.

5 Conclusion

A rate equation model was used to study a one-end-pumped Yb^{3+}-doped GG+IAG fiber laser. Unlike conventional fiber, the GG+IAG fiber has leakage loss and high absorption. Consequently, the output threshold is higher than that of a conventional fiber laser. Meanwhile, the operation length is much shorter. With appropriate operation length, the fiber could ensure robust single-mode operation with a large mode area. However, if the fiber length is either too

short or too long, it may have no single-mode output. Other characteristics of Yb^{3+}-doped GG+IAG fiber, such as mirror reflectivity, are also respected. All of these significances may provide some insights for later experiments.

Appendix

The signal power propagation can be described by $P_s^+(z) = P_s^+(0) \exp[(g_s - \alpha_s')z]$, in which g_s is the gain coefficient of the GG+IAG fiber laser, and α_s' includes both scatting and leakage losses. Consequently, the effective gain coefficient of the signal is $g_s' = g_s - \alpha_s'$, illustrated by $g_s' = \frac{1}{z} \ln(\frac{P_s^+(z)}{P_s^+(0)})$.

References

1. A.E. Siegman, J. Opt. Soc. Am. A **20**, 1617 (2003)
2. A.E. Siegman, Y. Chen, V. Sudesh, M.C. Richardson, M. Bass, P. Foy, W. Hawkins, J. Ballato, Appl. Phys. Lett. **89**, 251101 (2006)
3. A.E. Siegman, J. Opt. Soc. Am. B **24**, 1677 (2007)
4. Y. Chen, V. Sudesh, T. McComb, M.C. Richardson, M. Bass, J. Ballato, J. Opt. Soc. Am. B **24**, 1683 (2007)
5. V. Sudesh, T. McComb, Y. Chen, M. Bass, M. Richardson, J. Ballato, A.E. Siegman, Appl. Phys. B **90**, 369 (2008)
6. Y. Chen, T. McComb, V. Sudesh, Opt. Lett. **32**, 2505 (2007)
7. A. Hardy, R. Oron, IEEE J. Quantum Electron. **33**, 307 (1997)
8. I. Kelson, A.A. Hardy, IEEE J. Quantum Electron. **34**, 1570 (1998)
9. J. Zhou, J. Chen, X. Li, G. Wu, W. Jiang, C. Shi, Y. Wang, Opt. Express **14**, 3427 (2006)
10. R. Sims, V. Sudesh, T. McComb, Y. Chen, M. Bass, M. Richardson, A.G. James, J. Ballato, A. Siegman, in *Advanced Solid-State Photonics*, Denver, Colorado, 2009, Fiber Lasers and Bulk Solid-State Lasers: Poster Session III, paper WB3
11. I. Kelson, A.A. Hardy, J. Lightw. Technol. **17**, 891 (1999)